Time dependent density functional theory study of the near-edge x-ray absorption fine structure of benzene in gas phase and on metal surfaces

Frans A. Asmuruf and Nicholas A. Besley[a)]
School of Chemistry, University of Nottingham, University Park, Nottingham NG7 2RD, United Kingdom

(Received 4 June 2008; accepted 11 July 2008; published online 13 August 2008)

The near-edge x-ray absorption fine structure of benzene in the gas phase and adsorbed on the Au(111) and Pt(111) surfaces is studied with time dependent density functional theory. Excitation energies computed with hybrid exchange-correlation functionals are too low compared to experiment. However, after applying a constant shift the spectra are in good agreement with experiment. For benzene on the Au(111) surface, two bands arising from excitation to the $e_{2u}(\pi^*)$ and $b_{2g}(\pi^*)$ orbitals of benzene are observed for photon incidence parallel to the surface. On Pt(111) surface, a broader band arises from excitation to benzene orbitals that are mixed with the surface and have both σ^*(Pt–C) and π^* characters. © *2008 American Institute of Physics*.
[DOI: 10.1063/1.2967190]

I. INTRODUCTION

Near-edge x-ray absorption fine structure (NEXAFS) spectroscopy is a powerful technique for investigating the electronic and geometric structures of molecules adsorbed on surfaces. In recent years, NEXAFS has benefited from advances in intensity and resolution obtainable from synchrotron sources, which have resulted in spectra with greater structure that are more rich in information. The adsorption of benzene on metal surfaces is a prototypical problem that has been studied extensively, and NEXAFS spectra have been reported for benzene adsorbed on several metal surfaces.[1–5]

The NEXAFS spectroscopy of benzene is dominated by an intense π^* resonance. From measurements with the polarization of the incident radiation orthogonal and parallel to the surface, it has been established that benzene lies parallel to the surface. However, the measured spectra vary between different surfaces. For example, the NEXAFS spectra of benzene adsorbed on Pt(111) and Au(111) differ significantly, reflecting the different natures of the bonding to the surface.[4,5] Benzene is physisorbed on the Au(111) surface, and the spectrum for benzene adsorbed on Au(111) is similar to the spectrum for a benzene multilayer. The π^* resonance occurs at 285.1 eV and is intense at grazing photon incidence and absent at normal photon incidence. A second weaker band at 289.3 eV is also evident. At normal photon incidence, weak features at 287 eV can be distinguished. Benzene is chemisorbed on the Pt(111) surface, and the resulting spectrum shows a broad, less intense feature with two distinct peaks. This change has been attributed to the hydridization of the π^* orbitals with the metal electronic states.[4] The variation in intensity of this feature with the photon angle of incidence indicated a bending of the C–H bonds out of the plane of the benzene ring. For normal photon incidence, a weak broad feature centered at approximately 287 eV can be distinguished.

Theoretical calculations are useful in the analysis and interpretation of experimental spectra. Such calculations can assign spectral bands and provide a link between the observed spectral features and the underlying molecular structure. There are several approaches to computing NEXAFS spectra. These include multiple scattering X_α methods[6] and static exchange (STEX) calculations.[7] Within density functional theory (DFT), core-excited states can be computed with a Δ Kohn–Sham self-consistent field approach. In this method, the core-excited state is computed by imposing a constraint of a single occupancy of a core orbital within the self-consistent field calculation to prevent the variational collapse. For calculations of NEXAFS spectra comprising many core-excited states, this method is inefficient since it requires individual Kohn–Sham calculations for each excited state. The problem of optimizing individual states is avoided in the transition potential method.[8] In this approach the ground and excited states are determined within a single calculation in which the core level has half an electron removed, capturing a balance between final and initial states. Alternatively, NEXAFS spectra can be computed using time dependent DFT (TDDFT). This can be achieved efficiently by limiting the single excitation space to include only excitation from the relevant core orbitals.[9,10] Recently, a resonant converged complex polarization propagator method has been implemented[11] and applied to study NEXAFS.[12,13] The shift in the computed spectra compared to experiment was attributed to a self-interaction error, and a self-interaction correction was proposed.[14]

The application of theoretical techniques to study the NEXAFS spectroscopy of molecules on surfaces is relatively uncommon, but a small number of groups have addressed this problem.[8,15–22] Horsley *et al.* studied the NEXAFS of ethene on the Pt(111) surface,[15] and Pettersson and coworkers have studied the x-ray absorption and x-ray emission spectra of small molecules on the Cu(110) surface using STEX and transition potential methods.[8,17,18,20,21] In a study of *n*-octane, it was shown that resonances arising from exci-

[a)]Electronic mail: nick.besley@nottingham.ac.uk.

tation to Rydberg states were strongly quenched and there is a significant hybridization of molecular valence states with the metal bands.[20] In this contribution, we investigate the calculation of the NEXAFS spectra of benzene in the gas phase and adsorbed on Au(111) and Pt(111) surfaces with TDDFT.

II. COMPUTATIONAL DETAILS

TDDFT is well established for computing valence excited states and has been extended to the efficient computation of core-excited states.[9,10] Within the Tamm–Dancoff approximation[23] (TDA) of TDDFT, excitation energies and oscillator strengths are determined as the solutions to the eigenvalue equation,[24]

$$\mathbf{AX} = \omega \mathbf{X}. \tag{1}$$

The matrix $\mathbf{A}$ is given by

$$A_{ia,jb} = \delta_{ij}\delta_{ab}(\varepsilon_a - \varepsilon_i) + (ia|jb) + (ia|f_{\mathrm{XC}}|jb), \tag{2}$$

where two-electron integrals are given in Mulliken notation,

$$(ia|f_{\mathrm{XC}}|jb) = \int d\mathbf{r}\, d\mathbf{r}'\, \psi_a^*(\mathbf{r})\psi_i(\mathbf{r})\frac{\delta^2 E_{\mathrm{XC}}}{\delta\rho(\mathbf{r})\delta\rho(\mathbf{r}')}\psi_j^*(\mathbf{r}')\psi_b(\mathbf{r}'), \tag{3}$$

and the convention of $i,j,\ldots$ denoting occupied orbitals and $a,b,\ldots$ denoting virtual orbitals are adopted. $\mathbf{X}$ describes the linear response of the Kohn–Sham density matrix in the basis of the unperturbed molecular orbitals, ε_i are the orbital energies, ω give the excitation energies, and E_{XC} is the exchange-correlation functional. The TDA of TDDFT was used in this work because it is within this formalism that we have implemented a restricted excitation subspace methodology used in this work. However, there is evidence to suggest that the TDA formalism may be more appropriate for describing the weak Pt–C bonds formed on chemisorption of benzene on the Pt(111) surface.[25,26]

The solution of the eigenvalue equation [Eq. (1)] is achieved using the iterative method of Davidson.[27] While efficient for valence states, this approach is inefficient for core-excited states. This results in the computation of core-excitation energies being computational prohibitive. A solution to this problem is to perform the TDDFT calculation within the subspace of single excitations involving excitations from the relevant core orbital(s). The following equation is solved[9,28]

$$\bar{\mathbf{A}}\mathbf{X} = \omega \mathbf{X}, \tag{4}$$

where

$$\bar{\mathbf{A}} = A_{\bar{i}a,\bar{j}b} \tag{5}$$

and $(\bar{i})$ represents a subset of the occupied orbitals. We have used this approach to study the NEXAFS (Ref. 10) and electronic[29,30] spectroscopy of a variety of molecules adsorbed on surfaces.

In this study, the surface is modeled with a small cluster of metal atoms and the effects of relatively are not accounted for. Two types of surface cluster, comprising one and three layers, are used. The simple one-layer cluster has 12 atoms, and the three-layer cluster has 22 atoms. While relatively small, the calculation of NEXAFS spectra for molecules adsorbed on the 22 atom cluster is computationally demanding because of the very large number of excited states required. However, earlier work has shown that NEXAFS spectra are less sensitive to cluster size than other properties such as binding energy.[16] Bilic *et al.* have reported a detailed study of the adsorption of benzene on a range of metal surfaces, including Au(111).[31] For the calculations presented here, the most stable structure predicted for benzene on Au(111) by Bilic *et al.* corresponding to benzene in a threefold hollow site is used. When physisorbed on Au(111), benzene retains its planar structure. On Pt(111), benzene can occupy threefold hollow or bridge sites. Structures for benzene in both threefold and bridge sites were adapted from the work of Morin *et al.*[32] For both binding sites, the surface atoms are fixed in position and benzene is strongly chemisorbed to the surface with six metal-carbon bonds formed. In both threefold hollow and bridge sites the hydrogens are distorted upward from the plane of the carbon ring. For the threefold site, the adsorbed benzene retains its sixfold rotational symmetry. For the bridge site, the carbons bonded to the "end" carbons are distorted upward to a greater extent than the other hydrogen atoms, and the sixfold rotational symmetry is lost. These structures are illustrated in Fig. 1.

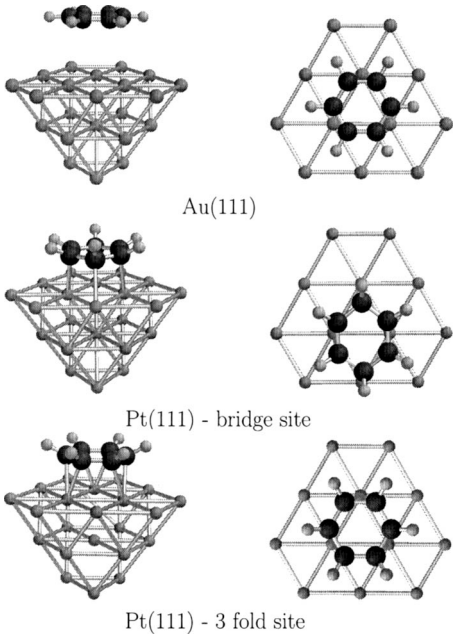

FIG. 1. Cluster models of benzene adsorbed on Au(111) and Pt(111) surfaces.

All calculations were performed with the Q-CHEM software package,[33] except the calculations with the CS00 functional,[34,35] which used the NWCHEM software.[36] The 6-311G* basis set was used for benzene, which was augmented with a set of Rydberg basis functions[37] placed at the center of the ring for some calculations. For the NEXAFS calculations of adsorbed benzene, the LANL2DZ basis set[38,39] was used for the gold and platinum atoms. Theoretical spectra are generated by representing the computed exci-

TABLE I. The largest and average errors in the excitation energies in eV and oscillator strengths (in parentheses) of the ten lowest core-excited states resulting from the truncation of the single excitation space.

Molecule	Largest error	Average error
N_2	0.01 (0.013)	0.00 (0.003)
C_2H_2	0.01 (0.009)	0.00 (0.002)
C_2H_4	0.02 (0.011)	0.01 (0.002)
H_2CO (C 1*s*)	0.01 (0.009)	0.00 (0.002)
H_2CO (O 1*s*)	0.01 (0.004)	0.00 (0.001)
HCl-1*s*	0.00 (0.000)	0.00 (0.000)
HCl-2*s*	0.05 (0.004)	0.01 (0.004)
SiH_4-1*s*	0.00 (0.000)	0.00 (0.000)
SiH_4-2*s*	0.04 (0.001)	0.01 (0.000)
PH_3-1*s*	0.01 (0.000)	0.01 (0.000)
PH_3-2*s*	0.07 (0.001)	0.02 (0.000)

tation energy and intensity of each electronic transition by a Gaussian function, a full width at half maximum of 0.4 eV was used for the spectra of gas phase benzene. Spectra for benzene adsorbed on the surfaces used a full width at half maximum of 1 eV.

III. RESULTS AND DISCUSSION

A. Benzene-gas phase

Before considering benzene, the effect of restricting the excitation space to include only excitations from core orbitals, Eq. (4), is examined. Table I shows the effect of introducing this restriction compared to the full excitation space for the ten lowest core-excited states for a range of molecules at the B3LYP/6-31+G* level of theory. The results show that this restriction introduces a very small error in the computed excitation energies and oscillator strengths. The average error is very small and is negligible relative to other errors inherent in the calculations. The largest error observed is for excitation from the 2*s* orbital of phosphorous in PH_3. In general, larger errors are observed for excitations from core 2*s* orbitals compared to the corresponding core 1*s* orbitals. This is expected since there is likely to be more mixing between this orbital and the virtual space. However, even the largest errors are relatively small. For benzene the excitations from the carbon 1*s* orbitals do not appear in the lowest 1000 roots. Therefore, it is difficult to assess directly the effect of restricting the excitation space; however, it would be expected that a similarly small error would be observed. Thus imposing that the restriction of only including excitations from the relevant core orbitals represents a practical and efficient method for computing NEXAFS spectra that can be incorporated easily into standard TDDFT codes.

The NEXAFS of benzene has been studied extensively.[1,12,40–45] In experiment four prominent bands are observed below the ionization threshold.[43] These are referred to as A, B, C and D, and occur at 285.2, 287.2, 287.9 and 289.2 eV, respectively. Peak A is the most intense peak and is assigned to excitation to e_{2u} orbitals, which correspond to the lowest π^* orbitals. However, there is less consensus in the literature over the assignment of the remaining peaks. Peak B has been assigned to Rydberg 3*s* (Ref. 43) or σ^* orbitals.[44,45] Similarly, peak C has been assigned to Rydberg 3*p* or 3*d* (Refs. 40 and 43) or σ^* orbitals.[44,45] Furthermore, peak D has been assigned to $b_{2g}(\pi^*)$ or Rydberg 3*d*, 4*s*, or 4*p* excitations.[40,43–45] Although most authors acknowledge these orbitals are of mixed character, and the assignment of the nature of these excitations will depend on the details of the calculation and on the precise definition of a Rydberg orbital adhered to.

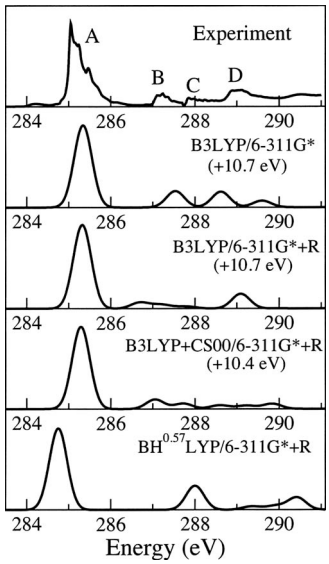

FIG. 2. Experimental and computed NEXAFS spectra of benzene in the gas phase. Experimental spectrum adapted from Ref. 43.

TDDFT spectra computed with a range of basis sets and exchange-correlation functionals are shown in Fig. 2. The experimental spectrum adapted from Ref. 43 is also shown. It has been observed previously that core-excitation energies computed with TDDFT with conventional functionals are too low.[46,47] For the B3LYP/6-311G* calculation, all excitation energies have been shifted by +10.7 eV to match experiment. The shifted spectrum is in good agreement with experiment, with an intense π^* band with three weaker bands predicted at higher energies. The 6-311G* basis set does not contain diffuse basis functions and is not designed for describing Rydberg states. Inclusion of a set of *s*, *p*, and *d* Rydberg basis functions located at the center of the benzene ring, denoted 6-311G*+R, does not affect the intense π^* band. However, the energies and intensities of the weaker bands are changed significantly, indicating some Rydberg character of these bands. For the B3LYP/6-311G*+R calculation, three weaker bands occur at 286.7, 287.2, and 289.1 eV (shifted by +10.7 eV). Orbitals derived from the B3LYP/6-311G* +R calculation are shown in Fig. 3. The intense band at 285.3 eV (shifted by +10.7 eV) corresponds to excitation to the e_{2u} orbitals, which are clearly π^* orbitals. The next band in the spectrum is much weaker and arises from an excitation to the a_{1g} orbital and corresponds to peak B. Previous work has assigned this orbital as 3*s*,[43] σ(C–C) bonding with antibonding C–H character,[44] and σ^*(C–C).[45] Overall, we find this orbital is most appropriately labeled a 3*s* orbital. The orbital has the correct symmetry, and Fig. 3 shows that it

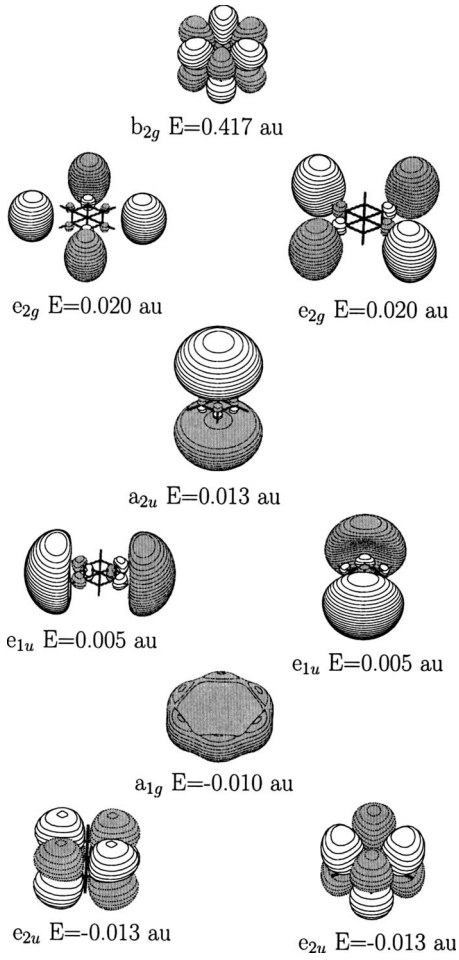

FIG. 3. Virtual orbitals of benzene in the gas phase.

looks like a 3*s* orbital, although it is perhaps not as diffuse as one might expect for a Rydberg orbital. The 3*s* orbital has two spherical nodal surfaces (not shown in Fig. 3). One of these surfaces does occur between the carbon and hydrogen atoms, which would reflect σ^*(C–H) character. However, there is no σ^*(C–C) character since there is no node between the carbon atoms. Peak C is weaker than peak B and is calculated to arise from excitations to the e_{1u} orbitals. These orbitals are shown in Fig. 3 and are best described as the in-plane Rydberg 3*p* orbitals. Again the orbitals also have a nodal surface along the C–H bonds, which reflects some σ^*(C–H) character. Above peak C a weak band arising from excitation to e_{2g} orbitals and a more intense band corresponding to excitation an a_{2u} orbital. The e_{2g} orbitals are best described as Rydberg 3*d* orbitals, while the transition to the a_{2u} orbital corresponds to peak D and is best described as an out-of-plane Rydberg *p* orbital. Previous work has assigned peak D to the $b_{2g}(\pi^*)$ orbital. However, in our calculations this orbital is found at a significantly higher energy.

For the B3LYP/6-311G*+R calculation, the weak (Rydberg) bands are two low in energy with respect to the π^* band. It is well known for valence excited states that functionals such as B3LYP underestimate the excitation energies of Rydberg states. This can be corrected by the use of the CS00 asymptotically corrected (AC) functional.[35] The NEXAFS spectrum computed with B3LYP with an asymptotic correction is also shown in Fig. 2. The AC functional does not correct the large underestimation of the excitation energies, but does shift the Rydberg bands to higher energies relative to the π^* band. Once shifted by +10.4 eV, the resultant spectrum is in reasonable agreement with experiment. The peaks at B, C, and D are computed to lie at 287.1, 287.7, and 288.6 eV, respectively. This compares to experimental values of 287.2, 287.9, and 288.9 eV. The largest deviation from experiment is the intensity of band D is underestimated.

The origin of the error that results in the large underestimation of the computed core-excitation energies is analogous to the error observed for charge transfer states and is not corrected by an AC functional. This error has been discussed extensively in the literature and has been termed the electron transfer self-interaction error[48] and arises when there is little spatial overlap between the occupied and virtual orbitals involved in the excitation. Since core orbitals are compact and localized on the nuclei, there is little overlap between these orbitals and typical virtual orbitals, such as π^*. Consistent with this analysis, greater accuracy can be achieved by increasing the proportion of Hartree–Fock exchange in the functional. A spectrum was computed with the $BH^{0.57}LYP$ functional.[10] This functional was developed to reproduce the $1s \rightarrow \pi^*$ excitations in acetylene, ethylene and benzene. The calculation predicts the π^* band to lie at 284.7 eV, which is in good agreement with experiment and it is no longer necessary to shift the spectrum. However, the weaker bands at higher energy are not described less well by this functional and are predicted to lie at energies that are too high relative to the π^* band.

B. Benzene on Au(111) and Pt(111)

Figure 4 shows experimental and computed spectra for benzene adsorbed on the Au(111) surface. The experimental spectrum for incident radiation parallel to the surface shows an intense peak at 285.3 eV with a weaker band at 289.2 eV. For this system, the lowest lying virtual orbitals correspond to the orbitals of the metal cluster. To reduce the cost of the calculation, the excitation space is reduced further, and excitation to the lowest ten virtual orbitals is excluded. This has negligible effect on the position and intensity of the lowest π^* band. In order to aid comparison with experiment, the computed spectra are shifted by +10.7 eV, the value derived from the gas phase calculations. Computed spectra are shown for incident radiation parallel and perpendicular to the surface.

All calculations use the B3LYP exchange-correlation functional and the LANL2DZ basis set for the gold atoms. The 6-311G*+R basis set for benzene in conjunction with the one-layer surface calculation predicts an intense band arising from excitations to the $e_{2u}(\pi^*)$ orbitals of benzene is at 285.4 eV (when shifted by +10.7 eV) with a weaker band arising from excitation to the $b_{2g}(\pi^*)$ orbitals of benzene at 290 eV. The relative positions and intensities of these bands are in good agreement with experiment. In comparison to the spectra of benzene in the gas phase, there is no evidence of excitation to Rydberg states in the spectrum for grazing photon incidence. The absence of Rydberg states in the spectrum

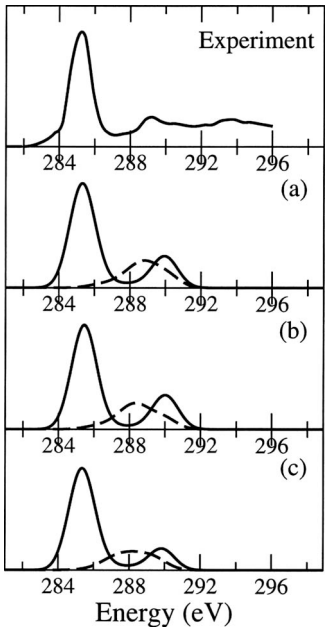

FIG. 4. Experimental and computed NEXAFS spectra of benzene adsorbed on Au(111). (a) B3LYP/6-311G*+R calculation with a one-layer surface cluster, (b) B3LYP/6-311G* calculation with a one-layer surface cluster, and (c) B3LYP/6-311G* calculation with a three-layer surface cluster. Solid lines: grazing photon incidence; broken lines: normal photon incidence. All calculated spectra have been shifted by +10.7 eV. Experimental spectrum for grazing photon incidence adapted from Ref. 4.

is likely to be a result of the presence of the surface resulting in the Rydberg states being destabilized relative to the valence states as observed for molecules in solution.[49,50] Removing the Rydberg basis functions from the basis set and using the larger cluster surface model has little effect on the computed spectra, although there is a little reduction in the intensity of the $b_{2g}(\pi^*)$ band. For incident radiation normal to the surface, the calculations predict a weak band at about 288.5 eV. For the three-layer cluster, this band occurs at a slightly lower energy of 285.1 eV. In experiment, there is some evidence for a weak feature in this region for normal incidence. In terms of gas phase benzene, this band arises from excitation to the a_{1g} orbital, which is best described as the Rydberg $3s$ orbital, although it does have some $\sigma^*_{\text{C–H}}$ character. The relative compactness of this Rydberg state results in its continued presence in the NEXAFS region on adsorption.

Figure 5 shows the experimental and calculated spectra for benzene adsorbed on the Pt(111) surface. Spectra have been calculated for both bridge and threefold binding sites. All calculations use the B3LYP exchange-correlation functional in conjunction with the 6-311G* basis set for benzene and LANL2DZ basis set for the platinum atoms. For grazing photon incidence, the calculations predict a broad band centered at 285.8 eV (shifted by +10.7 eV). For the one-layer surface cluster, two distinct peaks can be distinguished in this band. A further band at higher energy is also evident in the computed spectra. Overall, the predicted spectra between the bridge and threefold sites are similar. Some small differences are predicted, in particular, the higher energy band occurs at a slightly higher energy for the threefold site. The broad band arises from excitation to a number of low lying

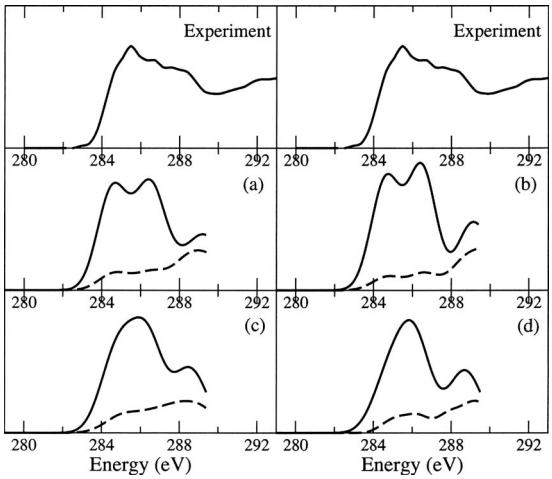

FIG. 5. Experimental and computed NEXAFS spectra of benzene adsorbed on Pt(111). (a) Bridge site on a one-layer surface cluster, (b) threefold site on a one-layer surface cluster, (c) bridge site on a three-layer surface cluster, and (d) threefold site on a three-layer surface cluster. Solid lines: grazing photon incidence; broken lines: normal photon incidence. All calculated spectra have been shifted by +10.7 eV. Experimental spectrum for grazing photon incidence adapted from Ref. 4.

virtual orbitals; the predominant contributions involve excitation to the orbitals shown in Fig. 6. The orbitals are clearly mixed between the benzene and surface, consistent with previous work on this system.[4] For ethene chemisorbed on Pt(111), the features observed in the NEXAFS spectra and underlying molecular orbitals have been discussed in detail.[15] Surprisingly, it was found that despite being bonded

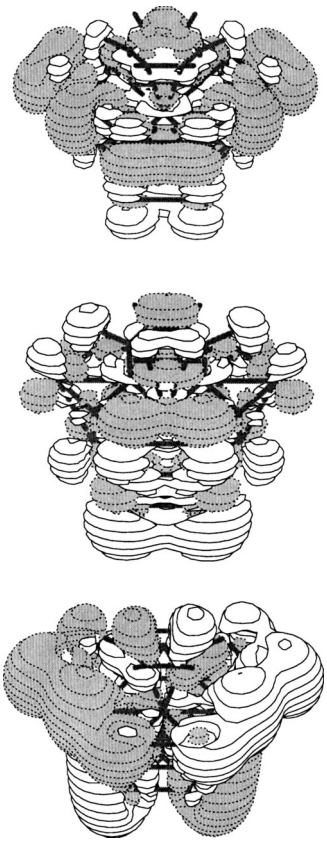

FIG. 6. Virtual orbitals of benzene adsorbed on Pt(111) in the threefold bonding site.

to the surface, the π^* orbital retained its identity. The resulting orbital was described as an antibonding combination of the ethene π^* orbital and the Pt d orbitals. Providing definitive labels for these orbitals is difficult, but chemically $\sigma^*_{\text{Pt–C}}$ orbitals would be expected. The orbitals would lie along the Pt–C bonds and should be observed for grazing photon incidence. The upper orbital in Fig. 6 is consistent with this. However, in terms of the benzene molecule, the lower two orbitals do have π^* character. So similar to ethene, some π^* orbitals are retained. At normal photon incidence, experiment predicts a weak feature at 286.5 eV.[4] All the computed spectra show a weak feature at this energy. Overall, the agreement with experiment is not as good as for benzene on the Au(111) surface. This reflects the much more complex bonding to the surface that occurs on the Pt(111) surface. However, the general features of the experimental spectrum are reproduced.

IV. CONCLUSIONS

The adsorption of benzene on metal surfaces is a prototypical problem in surface science, and high quality NEXAFS spectra have been reported in the literature.[4] Consequently, it provides a useful system to assess the performance of TDDFT for the calculation of NEXAFS spectra of molecules adsorbed on metal surfaces. For gas phase benzene, the excitation energies computed with TDDFT with hybrid functionals are too low compared to experiment. However, applying a constant shift to all excitation energies results in spectra that are in good agreement with experiment. The source of this discrepancy is not corrected by the use of an AC functional and is associated with the approximate local exchange in the hybrid functional. The use of a functional that has an increased fraction of Hartree–Fock exchange results in a spectrum for which a the application of a shift is not required; however, the agreement for the higher lying Rydberg bands is less good.

The NEXAFS spectra of benzene adsorbed on the Au(111) and Pt(111) surfaces has been computed with cluster models of the surface. For benzene adsorbed on the Au(111) surface, the computed spectra are in good agreement with experiment. For grazing photon incidence, the spectrum shows two bands that arise from excitation to the π^* orbitals of benzene and an absence of Rydberg bands. For normal photon incidence, a weaker band at 285.8 eV, corresponds to excitation to the 3s orbital of benzene. Benzene adsorbed on the Pt(111) is a much more complex system, and the agreement between experiment and theory is less good. For grazing photon incidence, the computed spectra show a broad band that is less intense than the π^* band observed on Au(111). These bands arise from excitation to virtual orbitals of benzene that are mixed extensively with the orbitals of the surface and have both $\sigma^*_{\text{Pt–C}}$ and π^* characters. Overall, while the accurate calculation of NEXAFS spectra for adsorbed molecules remains a challenge, TDDFT can provide a useful tool for understanding and interpreting NEXAFS spectra.

ACKNOWLEDGMENTS

F.A.A. would like to acknowledge the Papua Government for a Ph.D. studentship grant. The authors are also grateful to the University of Nottingham for access to its high performance computing facility.

[1] J. A. Horsley, J. Stöhr, A. P. Hitchcock, D. A. Newbury, A. L. Johnson, and F. Sette, J. Chem. Phys. **83**, 6099 (1985).
[2] A. C. Liu, J. Stöhr, C. M. Friend, and R. J. Madix, Surf. Sci. **235**, 107 (1988).
[3] A. C. Liu, C. M. Friend, and J. Stöhr, Surf. Sci. **236**, L439 (1990).
[4] K. Weiss, S. Gebert, M. Wühn, H. Wadepohl, and Ch. Wöll, J. Vac. Sci. Technol. A **16**, 1017 (1998).
[5] Ch. Wöll, J. Synchrotron Radiat. **8**, 129 (2001).
[6] J. A. Sheehy, T. J. Gil, C. L. Winstead, R. E. Farren, and P. W. Langhoff, J. Chem. Phys. **91**, 1796 (1989).
[7] H. Ågren, V. Carravetta, O. Vahtras, and L. G. M. Pettersson, Chem. Phys. Lett. **222**, 75 (1994).
[8] L. Triguero, L. G. M. Pettersson, and H. Ågren, Phys. Rev. B **58**, 8097 (1998).
[9] M. Stener, G. Fronzoni, and M. de Simone, Chem. Phys. Lett. **373**, 115 (2003).
[10] N. A. Besley and A. Noble, J. Phys. Chem. C **111**, 3333 (2007).
[11] P. Norman, D. M. Bishop, H. J. Aa Jensen, and J. Oddershede, J. Chem. Phys. **123**, 194103 (2005).
[12] U. Elkström and P. Norman, Phys. Rev. A **74**, 042722 (2006).
[13] U. Elkström and P. Norman, Phys. Rev. Lett. **97**, 143001 (2006).
[14] G. Tu, Z. Rinkevicius, O. Vahtras, H. Ågren, U. Elkström, P. Norman, and V. Carravetta, Phys. Rev. A **76**, 022506 (2008).
[15] J. A. Horsley, J. Stöhr, and R. J. Koestner, J. Chem. Phys. **83**, 3146 (1995).
[16] L. G. M. Pettersson, H. Ågren, O. Vahtras, and V. Carravetta, J. Chem. Phys. **103**, 8713 (1995).
[17] T. Triguero and L. G. M. Pettersson, Surf. Sci. **398**, 70 (1998).
[18] L. G. M. Pettersson, H. Ågren, Y. Luo, and L. Triguero, Surf. Sci. **408**, 1 (1998).
[19] M. Nyberg, J. Hasselström, O. Karis, N. Wassdahl, M. Weinelt, and L. G. M. Pettersson, J. Chem. Phys. **112**, 5420 (2000).
[20] K. Weiss, H. Öström, T. Triguero, H. Ogasawara, M. G. Garnier, L. G. M. Pettersson, and A. Nilsson, J. Electron Spectrosc. Relat. Phenom. **128**, 179 (2003).
[21] H. Öström, D. Nordlund, H. Ogasawara, K. Weiss, T. Triguero, L. G. M. Pettersson, and A. Nilsson, Surf. Sci. **565**, 206 (2004).
[22] C. Kolczewski, F. J. Williams, R. L. Cropley, O. P. H. Vaughan, A. J. Urquhart, M. S. Tikhov, R. M. Lambert, and K. Hermann, J. Chem. Phys. **125**, 034701 (2006).
[23] S. Hirata and M. Head-Gordon, Chem. Phys. Lett. **314**, 291 (1999).
[24] A. Dreuw and M. Head-Gordon, Chem. Rev. (Washington, D.C.) **1005**, 4009 (2005).
[25] Z.-L. Cai and J. R. Reimers, J. Chem. Phys. **112**, 527 (2000).
[26] M. E. Casida, F. Gutierrez, J. Guan, F.-X. Gadea, D. Salahub, and J.-P. Daudey, J. Chem. Phys. **113**, 7062 (2000).
[27] E. R. Davidson, J. Comput. Phys. **17**, 87 (1975).
[28] N. A. Besley, Chem. Phys. Lett. **390**, 124 (2004).
[29] N. A. Besley, J. Chem. Phys. **122**, 184706 (2005).
[30] N. A. Besley and A. J. Blundy, J. Phys. Chem. B **110**, 1701 (2006).
[31] A. Bilic, J. R. Reimers, N. S. Hush, R. C. Hoft, and M. J. Ford, J. Chem. Theory Comput. **2**, 1093 (2006).
[32] C. Morin, D. Simon, and P. Sautet, J. Phys. Chem. B **108**, 12084 (2004).
[33] Y. Shao, L. Fusti-Molnar, Y. Jung, J. Kussman, C. Ochsenfeld, S. T. Brown, A. T. B. Gilbert, L. V. Slipchenko, S. V. Levchenko, D. P. O'Neill, R. A. Distasio, Jr., R. C. Lochan, T. Wang, G. J. O. Beran, N. A. Besley, J. M. Herbert, Y. L. Lin, T. Van Voorhis, S. H. Chien, A. Sodt, R. P. Steele, V. A. Rassolov, P. E. Masleh, P. P. Korambath, R. D. Adamson, B. Austin, J. Baker, E. F. C. Byrd, H. Daschle, R. J. Doerksen, A. Dreuw, B. D. Dunietz, A. D. Dutoi, T. R. Furlani, S. R. Gwaltney, A. Heyden, S. Hirata, C.-P. Hsu, G. Kedziora, R. Z. Khalliulin, P. Kluzinger, A. M. Lee, M. S. Lee, W. Lian, I. Lotan, N. Nair, B. Peters, E. I. Proyhov, P. A. Pieniazek, Y. M. Rhee, J. Ritchie, E. Rosta, C. D. Sherrill, A. C. Simmonett, J. E. Subotnik, H. L. Woodcock III, W. Zhang, A. T. Bell, A. K. Chakraborty, D. M. Chipman, W. J. Hehre, A. Warshel, H. F. Schaefer III, J. Kong, A. I. Krilov, P. M. W. Gill, and M. Head-Gordon, Phys.

Chem. Chem. Phys. **8**, 3172 (2006).
[34] M. E. Casida, C. Jamorski, K. C. Casida, and D. R. Salahub, J. Chem. Phys. **108**, 4439 (1998).
[35] M. E. Casida and D. R. Salahub, J. Chem. Phys. **113**, 8918 (2000).
[36] E. Apr, T. L. Windus, T. P. Straatsma *et al.*, NWCHEM, A Computational Chemistry Package for Parallel Computers, Version 4.6, 2004, Pacific Northwest National Laboratory, Richland, Washington 99352-0999, USA.
[37] J. Lorentzon, P.-A. Malmqvist, M. Fülscher, and B. O. Roos, Theor. Chim. Acta **91**, 91 (1995).
[38] P. J. Hay and W. R. Wadt, J. Chem. Phys. **82**, 270 (1985).
[39] P. J. Hay and W. R. Wadt, J. Chem. Phys. **82**, 299 (1985).
[40] W. H. E. Schwarz, T. C. Chang, U. Seeger, and K. H. Hwang, Chem. Phys. **117**, 73 (1987).
[41] T. Yokoyama, K. Seke, I. Morisda, K. Edamatsu, and T. Ohta, Phys. Scr. **41**, 189 (1990).
[42] H. Ågren, O. Vahtras, and V. Carravetta, Chem. Phys. **196**, 47 (1995).
[43] E. E. Rennie, B. Kempgens, H. M. Köppe, U. Hergenhahn, J. Feldhaus, B. S. Itchkawitz, A. L. D. Kilcoyne, A. Kivimäki, K. Maier, M. N. Piancastelli, M. Polcik, A. Rüdel, and A. M. Bradshaw, J. Chem. Phys. **113**, 7362 (2000).
[44] R. Püttner, C. Kolczewski, M. Martins, A. S. Schlacter, G. Snell, M. Sant'Anna, J. Viefhaus, K. Hermann, and G. Kaindl, Chem. Phys. Lett. **393**, 361 (2004).
[45] C. Kolczewski, R. Püttner, M. Martins, A. S. Schlacter, G. Snell, M. Sant'Anna, K. Hermann, and G. Kaindl, J. Chem. Phys. **124**, 034302 (2006).
[46] A. Nakata, Y. Imamura, and H. Nakai, J. Chem. Phys. **125**, 064109 (2006).
[47] A. Nakata, Y. Imamura, and H. Nakai, J. Chem. Theory Comput. **3**, 1295 (2007).
[48] A. Dreuw and M. Head-Gordon, J. Am. Chem. Soc. **126**, 4007 (2004).
[49] N. A. Besley and J. D. Hirst, J. Phys. Chem. A **102**, 10791 (1998).
[50] N. A. Besley and J. D. Hirst, J. Am. Chem. Soc. **121**, 8559 (1999).